Cohesive Zone Model for Intergranular Slow Crack Growth in Zirconia and Ceramic: Influence of the water concentration and Microstructure

Bassem El Zoghbi[1,*], Rafael Estevez[1], Christian Olagnon[2]

[1] Laboratoire SIMAP, UMR CNRS 5266, Grenoble-INP, UJF, Université de Grenoble, 38402, France

[2] Laboratoire MATEIS, UMR CNRS 5510, INSA Lyon, Université de Lyon, 69621, France

* Bassem.El-Zoghbi@simap.grenoble-inp.fr

Abstract We describe intergranular *slow crack growth* (SCG) in Zirconia within a cohesive zone methodology. Stress corrosion being thermally activated, a rate and temperature dependent cohesive zone formulation is proposed and shown able to capture SCG. In the present study, the influence of microstructure in terms of anisotropic properties, the grain to grain disorientation, and the initial thermal stress state that originates from the ceramic processing are shown to determine the kinetics of SCG and the level of the load threshold below which no slow crack growth is observed. The influence of the water concentration (R.H.) on the magnitude of the minimum load threshold and on the kinetics of SCG is investigated. Ultimately, this work aims at providing reliable predictions in long lasting applications of ceramics.

Keywords Zirconia, Ceramic, Slow crack growth, Cohesive Zone, Humidity

1. Introduction

Zirconia has been one of the most important ceramics and one of the prominent mechanical properties used in various domains as thermal barriers, coatings, and in medical applications. Their intrinsic advantages are wear chemical resistance and inertness. When subjected to subcritical mechanical loads in presence of water, Zirconia is prone to a delayed damage mechanism called *slow crack growth* (SCG). This damage process is environmentally assisted by the diffusion and adsorption of water molecules in the crack tip or along the grain boundaries, which will reduced the energy required for failure. SCG is characterized by the variation of the crack velocity with load level. It is show experimentally [1, 2, 7] that beyond a load threshold K_0, SCG takes place at a velocity that increases with load (regime *I*). Regime *I* depends strongly on the load level, temperature and water concentration. This process is influenced by the environment. Chevalier et al. [2] showed experimentally the influence of water concentration and temperature on SCG and on the threshold K_0 in Zirconia polycrystals (see Fig. 1). Increasing the water concentration (cf. air 25°C vs water 25°C) induced a shift in the V-K_I curve with an increase in the crack velocity and a decrease in the magnitude of K_0. The same trend is observed with increasing temperature (cf. water 25°C vs water 75°C) with an additional decreasing of the threshold K_0. The slope of regime *I* of the V-K_I curve is not affected by the environment but the kinetics of SCG (velocity, K_0) are strongly dependent on the magnitude of the mechanical load, water concentration and temperature. In the present study, we aim at predicting the load threshold K_0, the regime *I* of the V-K_I curve and at providing insight of the origin of their variation with the water concentration.

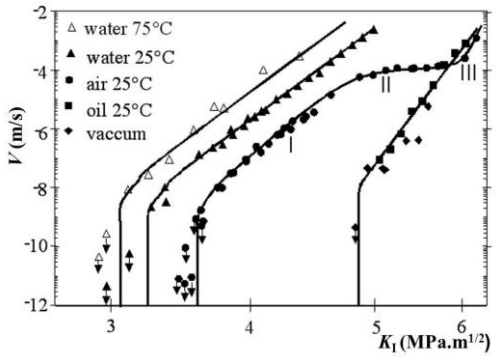

Figure 1. Slow crack growth in ceramics (Zirconia) velocity V versus the stress intensity factor K_I. The regime I shows a marked dependence with the relative humidity and temperature (data from [2]).

The mechanism underlying failure is described with a cohesive model that represents the reaction rupture process for SCG. Thus, a thermally activated formulation is adopted for the cohesive model (see Romero de la Oso et al. [2]). The formulation is shown in Romero de la Osa et al. [2-4] able to capture the regime *I*, the load threshold being related to the presence of initial stress (Romero de la Osa et al. [4]). We also investigate the influence of residual thermal stresses originating from the sintering process on the kinetics of SCG and on K_0. The influence of the water concentration on the kinetics of SCG and on the minimum threshold K_0 is also investigated.

2. Cohesive zone model for the reaction-rupture mechanism in ceramic

In this section, we present a cohesive zone model for the reaction-rupture mechanism underlying SCG in single and polycrystals ceramics. Michalske and Freiman [5] proposed an atomistic description accepted in the ceramic communities as a responsible for the process of SCG. They considered a bond of scilica in tension in presence of molecule of water that assists the breakdown of the bond to create two molecules of silanol. This model is reconsidered recently by Zhu et al. [6] by performing atomistic calculations. They observed that the reaction rupture is energetically favorable once a stress threshold is reached locally, with an activation energy that decrease with the applied stress. These observations are formulated with a cohesive zone methodology as Romero de la Osa et al. [3-4]. A thermally activated cohesive model is proposed where the damage opening rate for the description of the damage kinetics as

$$\dot{\Delta}_n^c = \dot{\Delta}_0 \exp\left(\frac{-U_0 + \beta\sigma_n}{k_B T}\right), \tag{1}$$

where $\dot{\Delta}_n^c$ is the opening rate between two surfaces in which damage occurs, U_0 is an activation energy, β has the dimension of a volume and σ_n is the traction normal to the cohesive surface. The pre-exponential term $\dot{\Delta}_0$ has the dimension of a velocity; k_B is the Boltzmann gas constant and T the absolute temperature.

Damage is triggered when $\sigma_n \geq \sigma_n^0$, σ_n^0 being a local load threshold. When the cumulated opening reaches a critical thickness Δ_n^{cr}, a crack is nucleated locally. The critical thickness Δ_n^{cr} is a material parameter, which is assumed to be about 1nm in crystalline material. According to Zhu et al. [6], the threshold stress σ_n^0 for the process to be energetically favorable ranging from 0 to 25% of the

athermal stress $\sigma_c = U_0/\beta$. For a traction smaller than threshold stress σ_n^0 neither damage nor reaction-rupture takes place. If the initial traction is higher than the threshold σ_n^0, the process will take place until a crack nucleates. For a traction smaller than the threshold stress σ_n^0 before the crack nucleation, the reaction-rupture stops.
In a finite element analysis, the related traction-opening is taken as

$$\dot{\sigma}_n = k_n(\dot{\Delta}_n - \dot{\Delta}_n^c), \tag{2}$$

where $\dot{\sigma}_n$ is the normal traction increment, $\dot{\Delta}_n$ is the prescribed opening rate, $\dot{\Delta}_n^c$ the damage opening rate, k_n is a stiffness that is taken large enough to ensure $\dot{\Delta}_n \approx \dot{\Delta}_n^c$ during the reaction rupture process. In this cohesive model formulation, we do not account for a contribution of the tangential mode in the reaction-rupture process. A simple elastic response is considered as

$$\dot{\sigma}_t = k_t\dot{\Delta}_t, \tag{3}$$

with $\dot{\sigma}_t$ is the tangential traction increment, $\dot{\Delta}_t$ the prescribed shear rate along the cohesive surface and k_t the tangential stiffness.
A quasi-static finite analysis is considered which uses a total Lagrangian description, the incremental shape of virtual work for this problem as (Romero de la Osa et al. [3,4])

$$\int_V \tau.\delta\dot{\eta}\, dV + \int_{Scz} \sigma_\alpha.\delta\dot{\Delta}_\alpha\, dS = \int_{\partial V} T.\delta\dot{u}\, dS, \tag{4}$$

where V and ∂V respectively represent the volume of the region in the initial configuration and its boundary, and S_{CZ} is the cohesive surface considered. The index α corresponds to the normal and tangential components in the cohesive formulation. In (Eq. 4), τ is the second Piola-Kirchhoff stress tensor, T the corresponding traction vector; $\dot{\eta}$ and ν are the conjugate Lagrangian strain rate and velocity. The governing equations are solved in a linear incremental fashion based on the rate form of (Eq. 4).

2.1. Calibration of cohesive zone parameters for Zirconia

We define a case study with an elastic bulk representing a single crystal (see Fig. 2a) under a static load. A linear elastic isotropic bulk is considered with an initial crack that is subjected to mode *I* and constant prescribed stress intensity K_I. Cohesive zone is inserted along the crack symmetry plane, where the principal stress is maximum. Small scale damage confined around the crack tip is assumed and the boundary layer approach is used to investigate mode *I* plane strain conditions. The mesh is refined around the crack propagation path (see Fig. 2b) and cohesive element of 1nm long is used. We prescribe a constant load in terms of stress intensity factor K_I as record the crack advance with time. We extract the velocity in the steady state regime and get one point in the V-K_I curve. By repeating this procedure, we are able to adjust the prediction with available experimental data [8]. The values of the Young modulus E^{iso} = 315 GPa and Poisson ratio ν^{iso} = 0.24 are derived from the cubic elastic constants of zirconia single crystals (see (Table 1). We adopt Δ_n^{cr} = 1nm, and based on Zhurkov [8] the energy barrier U_0 is of the order of the sublimation energy, with U_0 = 160kJ/mol. We still have to identify β and $\dot{\Delta}_0$, β controlling the slope of V-K_I and $\dot{\Delta}_0$ its position

(see Romero de la Osa et al. [3]). The identification of the parameters reported in Table 2, the predicted curve V-K_I being in agreement with the experimental data (see Fig. 3).

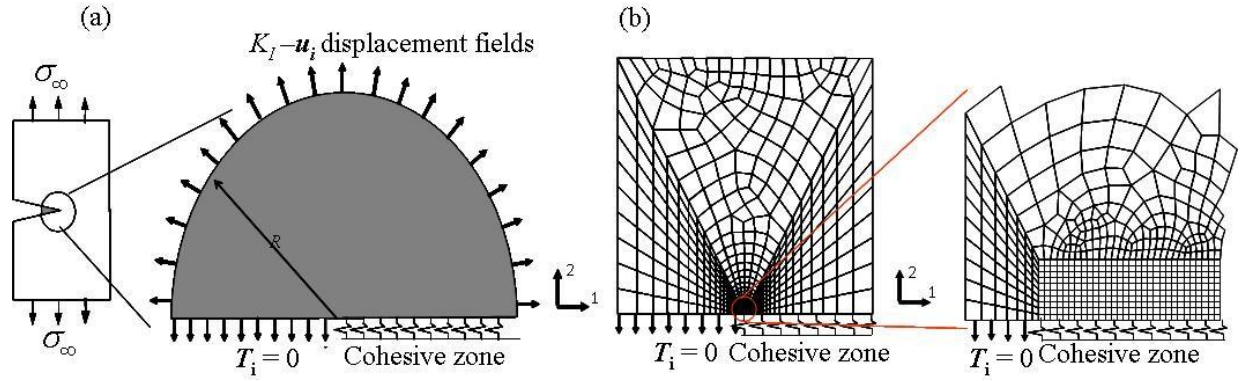

Figure 2. (a) Schematic description to model the zirconia SCG subjected to mode *I*, plain strain loading, (b) General view and zoom around the crack tip of the mesh used for the finite element analysis.

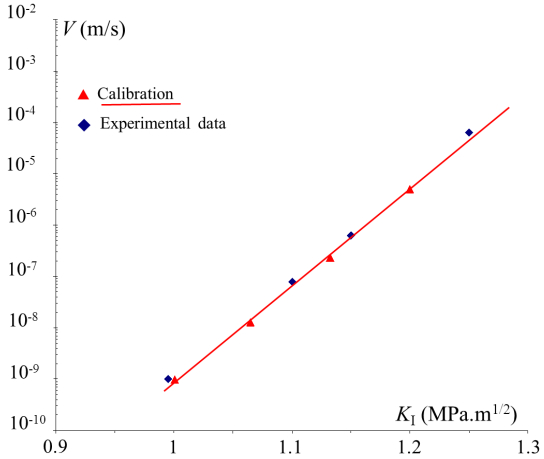

Figure 3. Calibration of cohesive zone parameters for zirconia based on experimental data [7] of SCG of zirconia single crystals

Table 1. Cubic elastic constants of zirconia single crystals (data from [9])

C_{11} (GPa)	C_{22} (GPa)	C_{33}(GPa)
430	94	64

Table 2. Parameters for the cohesive zone model for SCG in a zirconia single crystal

U_0 (kJ/mol)	Δ_n^{cr} (nm)	β (nm^3)	$\dot{\Delta}_0$ (mm/s)
160	1	0.027	3.2×10^{11}

3. Simulation and prediction of SCG in 2D zirconia polycrystal

We use the cohesive parameters indentified in the foregoing section to describe intergranular fracture under SCG in a polycrystal. We consider a granular zone composed by anisotropic hexagonal grains with random direction and with cohesive surfaces inserted along the grain boundaries. The problem formulation is depicted in Fig. 4. The polycrystalline zone is embedded in a continuum, homogeneous equivalent medium. An initial crack emerges in the granular zone. Along the remote boundary, the mode *I* K-fields are prescribed. Intergranular failure is allowed. The cubic elastic constants of zirconia grains are reported in Table 1 and the coefficients of thermal expansion are ($\alpha_1 = \alpha_3 = 10 \times 10^{-6}$ K^{-1}, $\alpha_2 = 11 \times 10^{-6}$ K^{-1}). The surrounding homogenous linear

isotropic bulk has a Young's modulus E = 315 GPa and Poisson's coefficient ν = 0.24, its isotropic coefficient of thermal expansion is taken as $\alpha = (2\alpha_1 + \alpha_2)/3$. In all cases, the polycrystal consists in a 8 × 8 grains with a grain diameter Φ_G = 0.8 μm. Two types of loading can be considered, a thermal and mechanical one. Firstly, we do not account to the initial thermal stresses originating during the cooling after sintering. We apply an instantaneous load in terms of K_I which is kept constant in time. The load is relaxed by intergranular failure. We consider a threshold stress σ_n^0 = 400 MPa corresponding to 4% of the athermal stress σ_c. In Fig. 5a, we have reported the distribution of the stress component σ_{yy} for various stages of the crack advance. The crack tip can be identified as the region with the highest stress concentration. We report the crack velocity for different load levels in Fig. 5b, that are compared with the experimental data of SCG in polycrystals for sintered Yttrium Stabilized Zirconia conducted by Chevalier et al. [7], for comparable grain sizes. We also report the curve V-K_I corresponding to the calibration of the cohesive zone for the zirconia single crystal. We observe that the predicted V-K_I curve is shifted toward larger load values for the polycrystal compared to the case of a single crystal. The slope of the V-K_I curve is comparable to the experimental data, but the predicted kinetics of SCG by simulation are faster than the experimental one. This difference may originate from 2D configuration in our simulation that promotes the crack advance in comparison with 3D configuration. Also, the initial thermal stress state is not considered here. Therefore, we now investigate their effect on SCG.

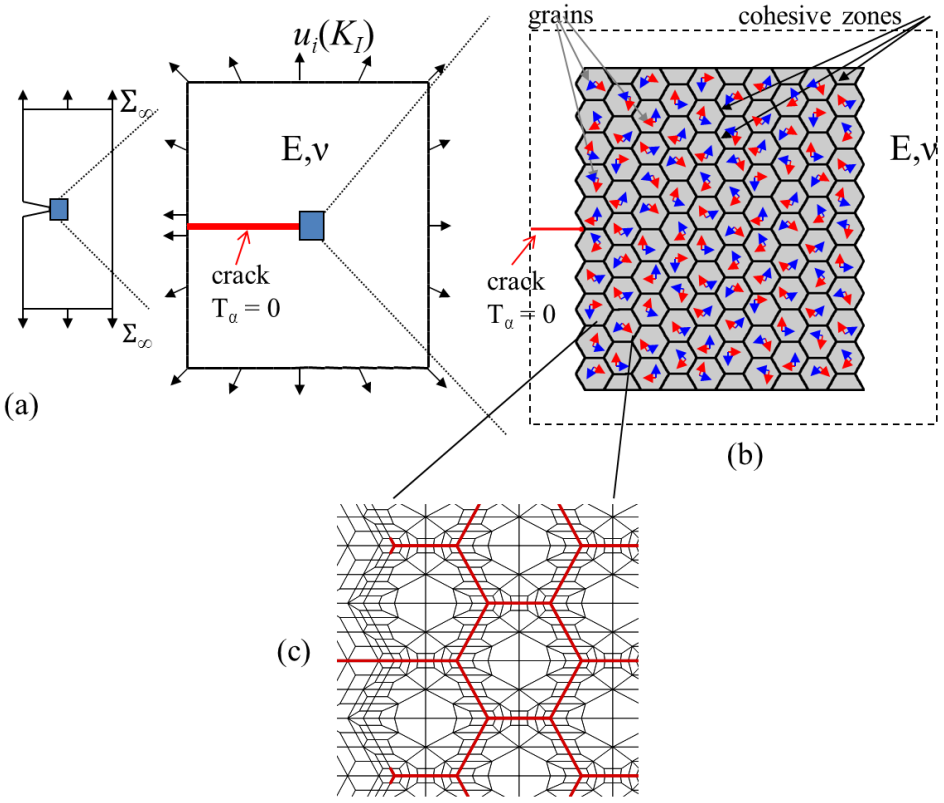

Figure 4. Small scale damage configuration used for the analysis of SCG in a 2D polycrystal

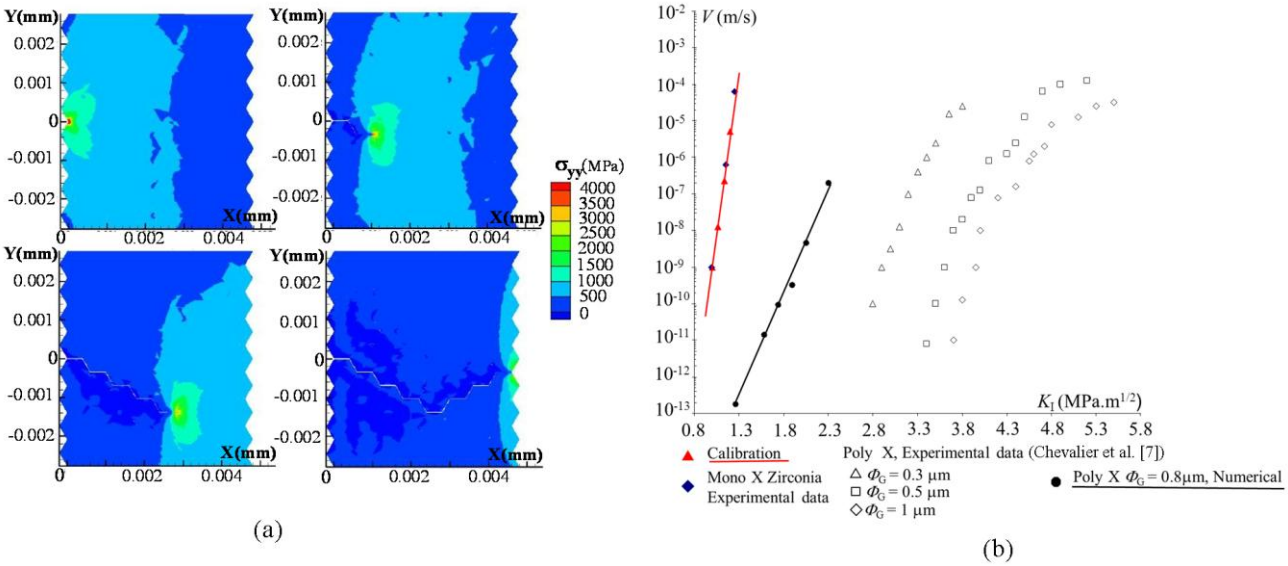

Figure 5. (a) Distribution of the stress σ_{yy} during crack propagation for a 2D polycrystal, (b) Comparison of the SCG plots V-K_I between the single crystal, the 2D polycrystal and Experimental data from [7]

3.1. Influence of the threshold stress σ_n^0 on the prediction of SCG

We now investigate the influence of threshold stress σ_n^0 corresponding to the initiation of the reaction-rupture mechanism on the SCG. Zhu et al [6] revealed the existence of a stress threshold σ_n^0 for the reaction-rupture process to be energetically favorable. The magnitude of σ_n^0 ranges is up to 25% the magnitude of the athermal stress σ_c. Therefore, we report in Fig. 6a the V-K_I curve for different values of σ_n^0 = 400, 900 and 1150 MPa corresponding to 4%, 9% and 12% of the athermal stress σ_c. We observe that the V-K_I curve is not affected by the variation of σ_n^0. However, σ_n^0 is particularly important in determining the threshold load K_0 below which no crack growth occurs. For the case with σ_n^0 = 400MPa, we do not observe a load threshold for SCG even for values as small as $K_I \approx 0.6$ MPa and $V \approx 10^{-16}$ m/s. For higher value of σ_n^0, a crack arrest is observed for K_0 = 0.9 MPa.mm$^{1/2}$ and σ_n^0 = 900 MPa. We observe that increasing the value of σ_n^0 increases the magnitude of K_0. The value of K_0 = 1.1 MPa.mm$^{1/2}$ is observed for σ_n^0 = 1150 MPa. During the relaxation if the normal traction becomes smaller than σ_n^0 before the crack nucleation, the reaction rupture stops. We report in Fig. 6b the cracks paths for arrested cracks corresponding to the threshold load K_0 below which no SCG occurs. These results show that with increasing the threshold stress σ_n^0, a threshold load of SCG can appear. It is related to the disorientation grain to grain that induce a reduction of the normal stress along the grain boundaries large enough for the normal traction σ_n becoming smaller than σ_n^0. In considering only these ingredients, we predict a threshold load of SCG in zirconia around 1MPa.m$^{1/2}$ for $\sigma_n^0 \approx 10\% \times \sigma_c$. We now investigate the influence of the thermal initial stress state on the magnitude of the threshold load K_0.

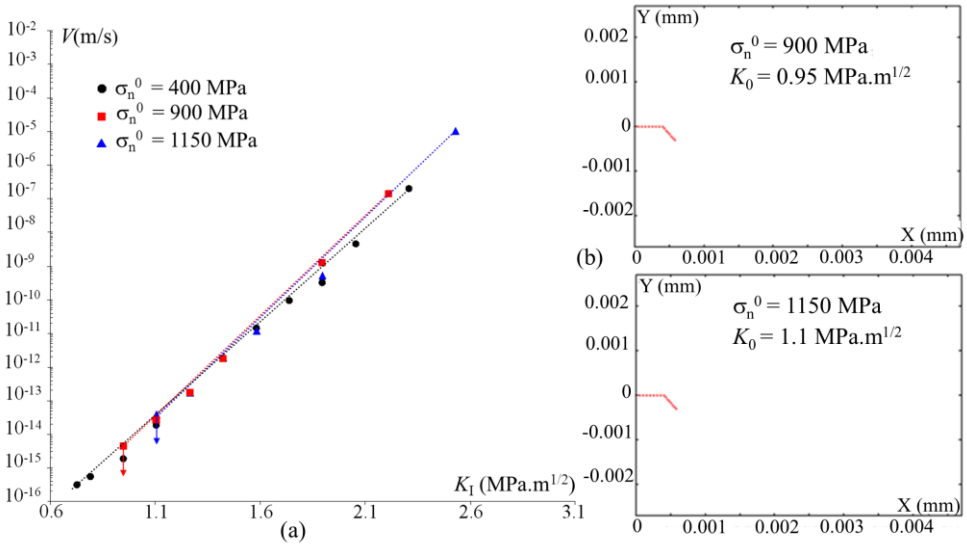

Figure 6. (a) Influence on the threshold stress of cohesive zone σ_n^0 and prediction of the V-K_I curve for Polycrystal of Zirconia with Φ_G = 0.8 μm, (b) Cracks paths for stopped cracks corresponding to the threshold load K_0 for σ_n^0 = 900 MPa and 1150 MPa.

3.2. Influence of thermal initial stresses on the prediction of SCG

During the sintering process, the material is cooled down from a temperature at approximately 1500 °C to the room temperature. This process will induce thermal stresses that originate from both the anisotropic coefficients of thermal expansion and anisotropic elastic constants of the grains. We consider the case with 8 × 8 grains, a grain size Φ_G of 0.8 μm for a uniform temperature cooling ΔT = -1500 K. The corresponding boundary conditions are presented in Fig. 7a, and the distributions of the stress component σ_{yy} reported in Fig. 7b, region under traction and compression are observed. From this initial state, we apply an external load K_I and we allow intergranular failure. For σ_n^0 = 400 MPa, 900 MPa and 1150 MPa, we report the corresponding V-K_I curves represented in Fig. 8a, 8b and 8c. For the three cases investigated, we observe that the presence of initial thermal stresses lead to a reduction of the crack kinetics. The curves V-K_I are shifted towards higher K_I values, preserving the slope of the curves corresponding to the polycrystals that are initially stress free. For the case with σ_n^0 = 400 MPa (see Fig. 8a) we observe that a threshold load K_0 now appears when we consider the initial thermal stresses. For σ_n^0 = 900 MPa and 1150 MPa, the magnitude of the threshold load of SCG increases when initial stresses are accounted for. We report in Fig. 9a, 9b and 9c the cracks paths for arrested cracks corresponding to the threshold load K_0 below which the crack is stopped for σ_n^0 = 400 MPa, 900 MPa and 1150 MPa respectively. The crack arrest is observed when the crack reaches a region where the compression is initially high enough with a locally stress level lower than threshold stress σ_n^0 of cohesive zone. The account of thermal initial stress contributes to a reduction of SCG kinetics. The magnitude of K_0 is also increased with initial thermal stress are accounted for. In the next section, we examine the influence of the water concentration on the predicted regime I and load threshold of SCG K_0.

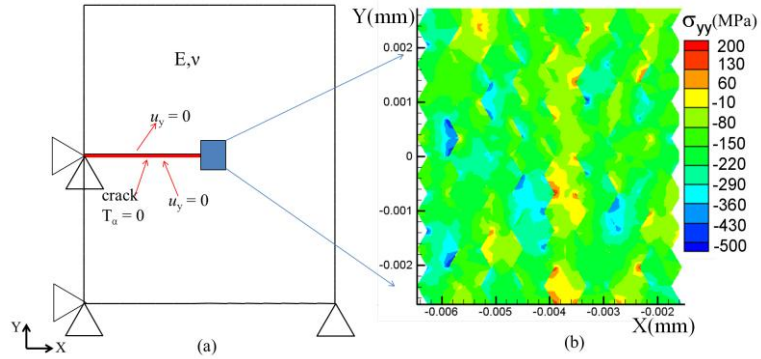

Figure 7. (a) Boundary conditions for thermal load, (b) Distribution of the stress component σ_{yy} in the polycrystal of zirconia with Φ_G = 0.8μm after a thermal cooling ΔT = -1500 K.

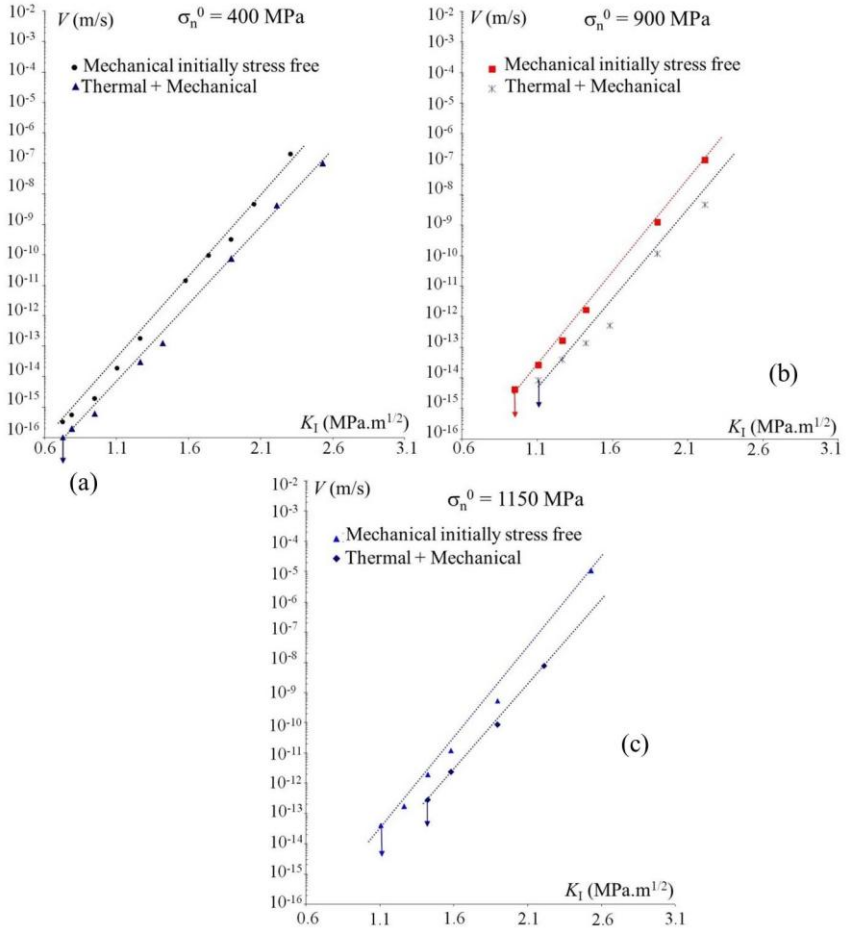

Figure 8. Influence of thermal initial stresses on the prediction of the V-K_I curves and K_0 for Polycrystals of Zirconia with Φ_G = 0.8 μm, (a) σ_n^0 = 400 MPa, (b) σ_n^0 =900 MPa and (c) σ_n^0 =1150 MPa.

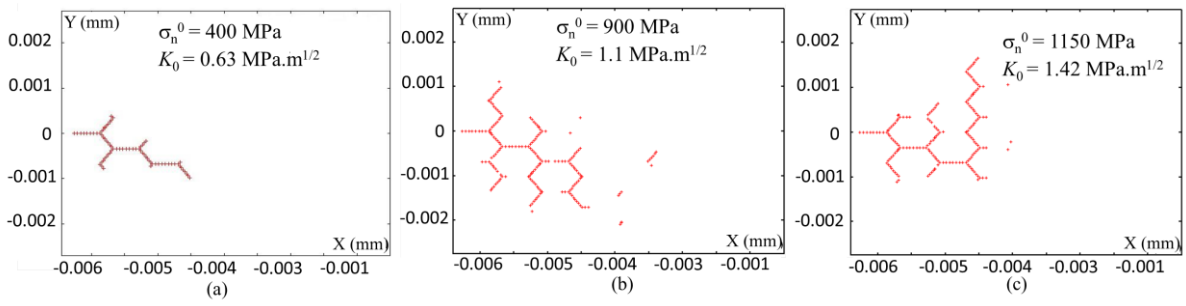

Figure 9. Cracks paths for stopped cracks, (a) σ_n^0 = 400 MPa , K_0 = 0.063 MPa.m$^{1/2}$, (b) σ_n^0 =900 MPa, K_0 = 1.1 MPa.m$^{1/2}$ and (c) σ_n^0 =1150 MPa, K_0 = 1.42 MPa.m$^{1/2}$.

3.3. Influence of water concentration on SCG

We investigate the influence of the water concentration (R.H.) on SCG in the zirconia polycrystal. We propose to account for the influence of R.H. by invoking a dependence of the energy barrier U_0 with the concentration of water molecules. By considering that an increase of R.H. results in decreasing the activation energy U_0(R.H.) that will facilitate the cracking. We consider an activation energy U_0 = 160 kJ/mol of the ambient air. We reduce this value by 10 % for an environment with more water and increase the reference value of U_0 by 10 % for a drier environment.
For each values of σ_n^0 = 900 MPa and 1150 MPa, we report the prediction in terms of V-K_I in Fig. 10a and Fig. 10b respectively. We observe that reducing the value of U_0 increases the value of the crack velocity for a given load K_I, while preserving the slope of the curve V-K_I. However, the dependence of threshold load K_0 in the water concentration is not affected by the variation of U_0(R.H.). This prediction is not in agreement with the experimental observations by Chevalier et al. [2] (see Fig. 1). We now examine the dependence of the threshold stress σ_n^0 of cohesive zone with the concentration of water molecules. When the water concentration increases, we now reduce U_0 by 10% (U_0 is increased by 10% for a drier environment). Therefore, we consider σ_n^0 = 900 MPa and U_0 = 160 kJ/mol as reference values in ambient air. The results in terms of V-K_I curves are reported in Fig. 11a. In Fig. 11b, we reported the results of the case with the references values of ambient air σ_n^0 = 1150 MPa and U_0 = 160kJ/mol. We observe that reducing the water concentration increases the threshold load K_0. These predictions are in agreement with the experimental observations in the influence of R.H on SCG by increasing the crack growth kinetics and reducing of threshold load of SCG K_0 with increasing R.H. In order to account to the first effect, we show that the dependence of energy barrier U_0 with R.H. takes account the variation of SCG kinetics with R.H. Nevertheless, it is important to take account the dependence of the threshold of activation of reaction-rupture mechanism σ_n^0 with R.H. At least this holds for the zirconia.

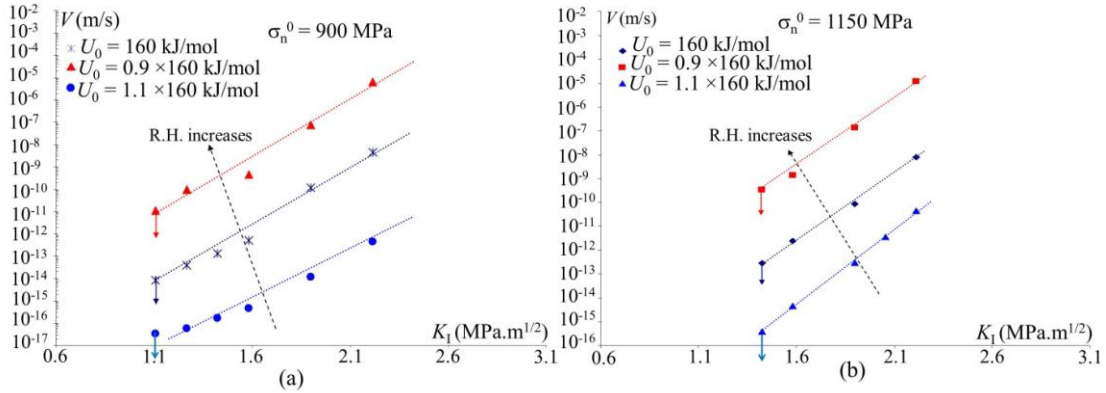

Figure 10. Influence of water concentration R.H. by its dependence with U_0 (R.H.) on the prediction of the V-K_I curves and K_0 for Polycrystals of Zirconia with Φ_G = 0.8 μm, (a) σ_n^0 = 900 MPa, (b) σ_n^0 =1150 MPa.

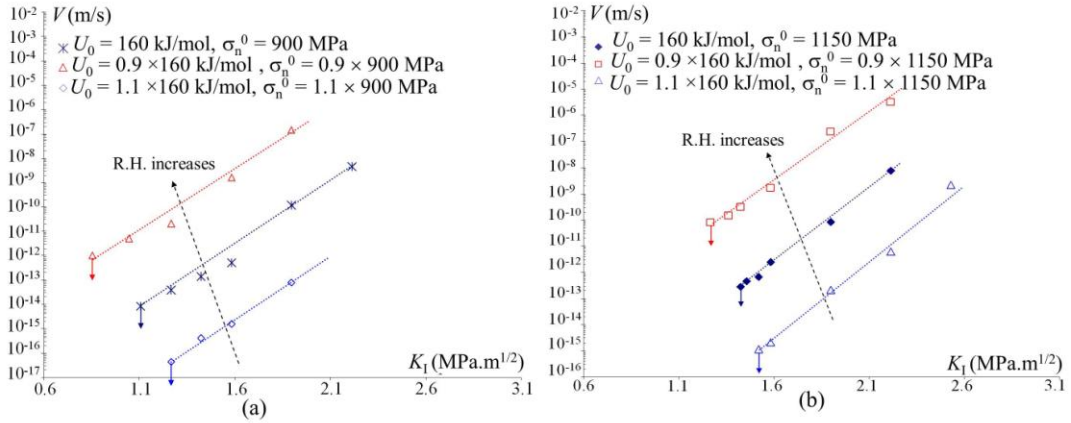

Figure 11. Influence of water concentration R.H. by its dependence with σ_n^0 (R.H.) and U_0 (R.H.) on the prediction of the V-K_I curves and K_0 for Polycrystals of Zirconia with Φ_G = 0.8 μm.

3. Conclusion

We have presented a calibration of the cohesive zone parameters for zirconia single crystal based on the cohesive zone description of Romero de la Osa et al. [3-4] for SCG in ceramics. The cohesive model is shown able to capture realistic experimental data of SCG in a single crystal. This calibration is then used to simulate intergranular failure in a 2D polycrystal. We have pointed on the influence of the stress threshold σ_n^0 for the reaction-rupture to be triggered on the prediction of the threshold load of SCG in a polycrystal. We have shown the influence of the initial thermal stresses related to processing on the kinetics of SCG and the magnitude of K_0. We also examined the influence of the water concentration on the prediction of the regime I and K_0 of SCG and showed that the water concentration can be accounted for with a dependence of the activation energy and traction threshold with the amount of water.

References

[1] K. Wan, S. Lathabai and B. Lawn, Crack velocity functions and thresholds in brittle solids in J. Am. Ceram.Soc., 1990, 6 259-68.
[2] J. Chevalier, C. Olagnon and G. Fantozzi, Subcritical crack propagation in 3y-tzp ceramics : static and cyclic fatigue, J. Am. Ceram. Soc., 1999, 82(11) :3129-3138.
[3] M. Romero de la Osa, R. Estevez, J. Chevalier, C. Olagnon, Y. Charles, L. Vignoud ,C. Tallaron, Cohesive zone model and slow crack growth in ceramic polycrystals, Int. J. Fract, 2009, 158(2) 157-167.
[4] M. Romero de la Osa, R. Estevez, J. Chevalier, C. Olagnon, Y. Charles, L. Vignoud ,C. Tallaron, Cohesive zone model for intergranular slow crack growth in ceramics : influence of the process and microstructure, Modell. Simul. Mat. Sci. Engng., 2011, 19:074009.
[5] T. A. Mischalske and S. W. Freiman, A molecular Mechanism for Stress Corrosion in Vitreous Silica, J. Am. Ceram. Soc., 66 284-8.
[6] T. Zhu and J. Li, X. Lin, S. Yip, Stress-Dependent Molecular Pathways of Silica-Water Reaction. J. Mech. Phys. Slolids, 2005, 53 1597-623.
[7] J. Chevalier and G. Fantozzi, Slow crack propagation in ceramics at the nano- and microscale : effect of the microstructure, Proceedings of the 8th Internaional Symposium on Fracture Mechanics of ceramics, held February 25 28, 2003, at the University of Houston, Texas.
[8] S. N. Zhurkov, Kinetics Concept of the Strength of Solids, J. Fract. Mech., 1965, 1 311-23.
[9] R. P. Ingel, D. Lewis, Elastic Anisotropy in Zirconia Single Crystals, J. Am. Soc., 1988, 74(4) 265-71.